Observation-Based Parameterisations of Major Source Functions, their Application in Extreme Conditions

Alexander V. Babanin
ababanin@swin.edu.au

Centre for Ocean Engineering, Science and Technology,
Swinburne University, Melbourne, Australia

Abstract. This paper is a review of recent progress in updating major source functions, used for spectral wave models at Swinburne University, following existing publications. These are wind input, whitecapping dissipation and negative input (interaction of waves with adverse wind). New parameterisations are based on measurements and observations, which revealed new physics previously unaccounted for. For extreme conditions, physics of the wind input and whitecapping dissipation terms exhibit additional features irrelevant or inactive at moderate weather.

In particular, the wave growth term was shown to be a nonlinear function of wave steepness. Additionally, the wave breaking was found to enhance the wind input. Relative reduction of the wind input at strong-wind/steep-wave conditions was observed, due to full flow separation found at such circumstances. At strong wind forcing, this causes saturation of the sea drag.

Spectral distribution of the whitecapping dissipation is the most elusive function to measure. Breaking of waves exhibits a clear threshold behaviour in terms of wave steepness. At a particular frequency, the breaking was demonstrated to cause energy damping in a broad spectral band above that frequency, and thus to bring about cumulative dissipative effect towards waves of smaller scales. It was found that at moderate winds the dissipation is fully determined by the wave spectrum whereas at strong winds it is a function of the wind speed.

Interaction of the waves with adverse wind is a necessary additional term if the above-mentioned wind input function is employed, since this function only describes forcing of waves by the following wind. Based on existing laboratory data, for a given wind speed magnitude of such negative input is 2.5 times smaller than the respective magnitude of positive wind input.

Qualitative and quantitative effects and properties of the observation-based source terms are parameterised. New parameterisations are presented in forms suitable for spectral wave models.

1. Introduction

Spectral evolution of the wind-generated wave field is commonly described by the radiative transfer equation (Hasselmann, 1960):

$$\frac{dF(\omega,\mathbf{k})}{dt} = I(\omega,\mathbf{k}) + N(\omega,\mathbf{k}) + D(\omega,\mathbf{k}) + B(\omega,\mathbf{k}) \qquad (1)$$

where the full derivative of the frequency (ω)-wavenumber ($\mathbf{k}$) spectrum $F(\omega,\boldsymbol{k})$ on the left-hand side is balanced by the sum of energy source I, sinks D and B, and spectral redistribution N terms on the right. Here, only energy terms for wind input I, dissipation in the water column D, bottom friction B, and four-wave nonlinear interactions N are mentioned, as they are usually the dominant terms. Equation (1) is the basic equation used in most of the phase-average numerical wave prediction models.

Until the last decade, experimental knowledge of the major source functions for wave models was very fragmental. They were largely based on theoretical argument combined with extensive tuning (e.g. Komen et al., 1994). Even when experimental data were available, these were either laboratory data or field measurements and observations conducted at light-to-moderate wind forcing, whose parameterisations are then extrapolated if extreme conditions are to be modelled. Such extrapolations are questionable, since physics of air-sea interaction at strong winds is expected and is known to be different (e.g. Babanin, 2011a,b).

In absence of reliable measurements of source functions, validations concentrated on reproducing wave growth curves. These are known reasonably well experimentally, and starting from seminal field observations of Mitsuyasu (1971) and JONSWAP (Hasselmann et al., 1973) their knowledge has continued to improve. The problem with such verifications, however, is that contributions of different source functions cannot be evaluated separately. What is validated is the balance of source terms in (1), while individual terms can be well of the scale (Babanin et al., 2010, Tsagareli et al., 2010). Potentially, this could lead to model failures or inaccuracy in conditions where such balance differs from the tuned situations.

Over the last decade, experimental knowledge of the source functions have improved significantly (e.g. The WISE Group, 2007), and this both produced quantitative guidance for the magnitude and parameterisations of the energy inputs/sinks and revealed new qualitative features of their behaviour as will be described in some detail in subsequent Sections. It is only recently, however, that the new knowledge and new physics started to make its way into the spectral models (Donelan, 2001, Babanin et al., 2007a, 2010, Ardhuin et al., 2010, Filipot et al., 2010, Tsagareli et al., 2010) and even in operational forecasting (Ardhuin et al., 2010, Tolman et al., 2011, Zieger et al., 2011, Donelan et al., 2012, Rogers et al., 2012).

Attention to the experimentally-guided physics also brings about the need for testing and calibrating the source functions independently, based on physical constraints (Babanin et al., 2005, 2007a, 2010, Tsagareli et al., 2010, Rogers et al., 2012). If each function satisfies respective constraints, then once combined in a wave-forecast model they require little or no further tuning to satisfy the academic growth tests or real ocean-wave hindcasts (Zieger et al., 2011, Rogers et al., 2012).

The present paper is not a general analysis of the problem and of the state of the art of the wave modelling. It is rather a review of observation-based source functions developed or adopted at the Centre of Ocean Engineering, Science and Technology of Swinburne University for spectral modelling, in collaboration with colleagues from Australia and overseas. In this regard, we should separate the experimentally observed phenomena of the energy/momentum exchanges in the wind-wave-ocean system and their parameterisations. The parameterisations, i.e. mathematical expressions for the source terms employed by the models, can differ between the models or model versions, until explicit theoretical description of the processes become available, but they all have to accommodate experimentally observed characteristics of these physical terms, in order for the models to conform closely with physical reality. For example, formulations for the new whitecapping dissipation terms in Young and Babanin (2006) and in Ardhuin et al. (2010) are different, but they both contain the important new features of the threshold behaviour for dissipation due to wave breaking and of the cumulative dissipation at small scales in the spectrum, and in this respect both source terms are consistent with observations.

The source functions discussed here are the wind input, whitecapping dissipation and negative input (interaction of waves with adverse wind). The first two are obtained in the course of Lake George field experiment (Young et al., 2005). Negative input is introduced according to laboratory experiments of Donelan (1999) with the following and adverse winds.

2. The observation-based source functions

The Lake George field experiment was designed to study the spectral balance of the source terms for wind-generated waves in finite water depth (Fig. 1). The measurements were made from a shore-connected platform at varying water depths from 1.2 m down to 20 cm. Wind conditions and the geometry of the lake were such that fetch-limited conditions with fetches ranging from approximately 10 km down to 1 km prevailed. The resulting waves were intermediate-depth wind waves with inverse wave ages, measured by the ratio of wind speed at 10 m height above the sea level, U_{10} to the phase speed of the dominant (spectral peak) waves, c_p in the range of $1 < U_{10}/c_p < 8$. The range is very broad and includes extreme wind forcing at the upper end.

The atmospheric input, whitecap dissipation and bottom friction were measured directly and synchronously by an integrated measurement system (Young et al., 2005). In addition, simultaneous data on the directional wave spectrum, atmospheric boundary-layer profile and atmospheric and underwater turbulence were acquired. The contribution to the spectral evolution due to nonlinear interactions of various orders was investigated by a combination of bi-spectral analysis of the data and numerical modelling. The relatively small scale of the lake enabled experimental conditions such as the wind field and bathymetry to be well defined. The observations were conducted over a three-year period from September, 1997 to August, 2000, with a designated intensive measurement period (AUSWEX) carried out in August-September 1999. High data return was achieved (Young et al., 2005).

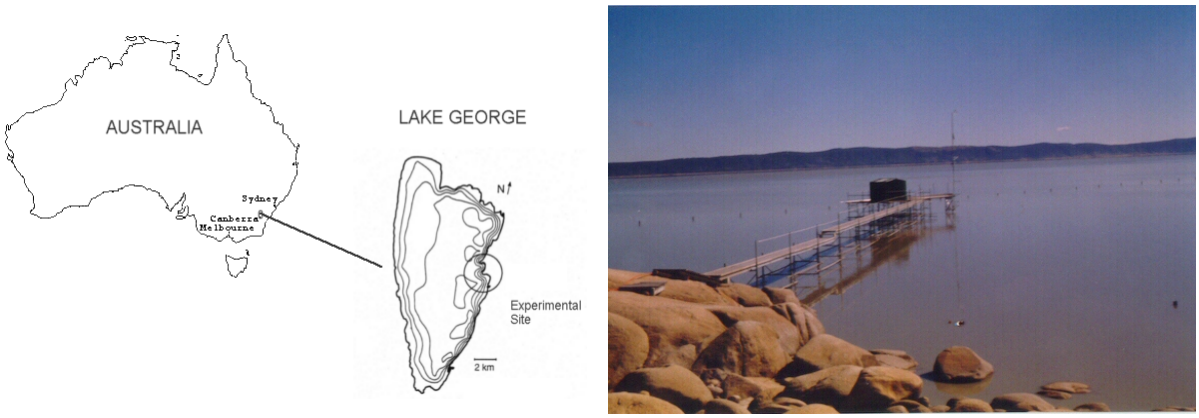

Figure 1. Location and view of the Lake George experimental site.

2.1. Wind input

Measurements of the wind input energy source I in (1) and its subsequent parameterisation as a function of wave spectrum and environmental forcing are described in a three-part series of papers by Donelan et al. (2005, 2006) and Babanin et al. (2007b). Technology of direct field measurements of the wave-induced pressure in the air flow over water waves is explained in Donelan et al. (2005). Nearly all of the energy delivered from wind to waves comes about through such wave-induced

pressure acting on the slopes of waves. The measurements of this kind are difficult and consequently rare, particularly in the field. In order to measure micro-scale oscillations of the induced pressure above surface waves, a high-precision wave-follower system was developed at the University of Miami, Florida and deployed at Lake George (Fig. 2). The principal sensing hardware included Elliott pressure probes, hot-film anemometers and Pitot tubes. The precision of the feedback wave-following mechanism did not impose any restrictions on the measurement accuracy in the range of wave heights and frequencies relevant to the problem. Thorough calibrations of the pressure transducers and moving Elliott probes were conducted. As a result of this study, it was shown for the first time that the response of the air column in the connecting tubes provides a frequency-dependent phase shift. This effect was not accounted for in previous measurements of this kind, but is very important for recovering the low-level induced pressure signal, particularly at higher frequencies.

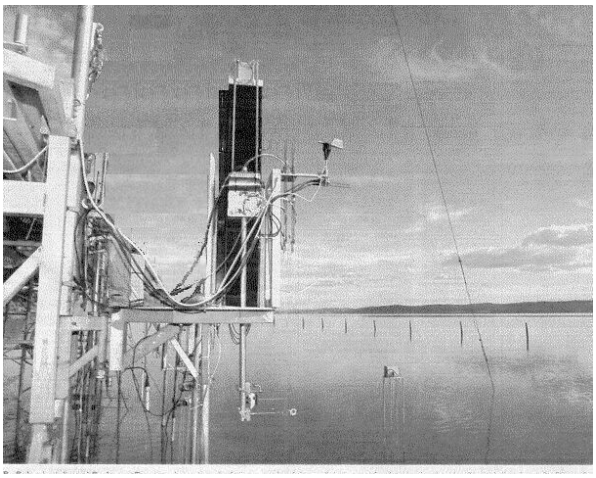

Figure 2. The wave follower shown positioned on the measurement bridge during AUSWEX. Three fingers with pressure probes can be seen on the shaft: the Elliott probe is at the bottom, with hot film anemometer above and the Pitot tube at the top.

The dimensionless growth rate of waves due to wind is often expressed in terms of the fractional energy increase γ, which is a spectral function

$$\gamma(\omega) = \frac{\rho_w}{\rho_a} \frac{1}{\omega F(\omega)} \frac{\partial F(\omega)}{\partial t}. \tag{2}$$

Here, ρ_w and ρ_a are densities of the water and air respectively. Once the growth rate function $\gamma(\omega)$ is known and the power spectrum $F(\omega)$ is available, the dimensional wind energy input is

$$I(\omega) = \rho_a \omega g \gamma(\omega) F(\omega) \tag{3}$$

where g is the gravitational constant.

Function for $\gamma(\omega)$, therefore, is the main experimental or theoretical task of the wind-input parameterisations. Note that $\gamma(\omega)$ is a spectral function, but is usually perceived not depending on the wave spectrum, i.e. the wind input spectrum $I(\omega)$ is a linear function of $F(\omega)$.

$\gamma(\omega)$ apparently depends on wind forcing, which is introduced through ratio of wind speed to phase speed of the wave $c(\omega)$. As the wind-speed proxy, either speed at a particular elevation above the

mean water level is used (for example, U_{10} or $U_{\lambda/2}$, the wind speed at the height of half of the wavelength λ), or friction velocity u_*. The friction velocity has dimension of speed, but is not a wind speed as such, it is a characteristic of wind stress (total momentum flux) τ:

$$\tau = \rho_a u_*^2 = \rho_a C_d U_{10}^2 \tag{4}$$

Here, C_d is the so called drag coefficient, an empirical property intended to convert the mean wind speed, usually available, into the momentum flux which is difficult to measure. Expression (4) implies some kind of proportionality between U_{10} and u_*, but in reality C_d is a growing function of the wind speed itself. Overall, it represents a complex structure of the atmospheric boundary layer and depends on very many features in the air-sea system near interface (e.g. Babanin and Makin, 2008). For the wind-input source term this is particularly essential as parameterisations in terms of U_{10}/c are not easily convertible into u_* / c. Functional form of the former is $\gamma \sim (U_{10} / c - 1)^n$, and for the latter it is $\gamma \sim (u_* / c)^n$. This is because the wind input tends to zero when wind speed approaches wave phase speed $U_{10} \to c$, whereas for the friction velocity this condition is $u_* \to 0$, i.e. momentum flux becomes zero.

2.1.1. Nonlinear dependence of the wind-wave energy exchange on wave spectrum

Previously reported measurements of the wave-induced air pressure were conducted in deep-water at conditions in which the level of forcing was rather weak: $U_{10} / c_p < 3$. As mentioned above, the data reported here, obtained during AUSWEX, have the range of $1 < U_{10} / c_p < 8$.

At Lake George, the propagation speeds of the dominant waves were limited by depth and, if the waves reached this limit, they were correspondingly steep. This provided the authors with a variety of wave slope values usually unavailable for direct observations outside laboratory conditions and thus enabled an investigation of a wave-steepness effect on the wind-wave energy exchange. The wave steepness is further characterised by product *ak* where *a* is the wave amplitude.

This wider range of forcing and concomitant wave steepness revealed some new aspects of the rate of wave amplification by wind (Donelan et al., 2006). These effects are illustrated in Fig. 3.

The measured growth rates for all the cases are shown in the top panel of Fig. 3. Most of previous parameterisations of the spectral growth rates implicitly assume a concept of self-similar sheltering, in which the geometry of the streamline pattern is preserved however steep the waves or strong the forcing is. This would lead to a linear relationship between γ and $(U_{\lambda/2} / c - 1)^2$. Obviously, the Lake George data in this panel, with their variety of wave-steepness and wind-force conditions, do not support such simple relationship. Data cluster in three separate groups, with no joint dependence of γ on $(U_{\lambda/2} / c - 1)^2$. If γ-on-$(U_{\lambda/2} / c - 1)^2$ relationships within individual groups were considered, the respective dependences bring γ down to zero while wind forcing is still very strong which makes no physical sense.

The slope, *s* of the relationship

$$\gamma = s(U_{\lambda/2} / c - 1)^2 \tag{5}$$

is the so-called sheltering coefficient and it is the product of the normalised (via the potential flow solution) pressure amplitude at the wavelength of the wave being forced and the sine of the phase shift of the pressure pattern relative to potential flow (in anti-phase with surface elevation). However, as illustrated in Donelan et al. (2006) the streamline geometry does not preserve its similarity having both the shift in phase and the normalised pressure amplitude related to wave steepness. The asymptotic value of both of these appears to approach the potential flow values of 0 and 1, respectively, as steepness *ak* approaches zero, which makes perfect physical sense.

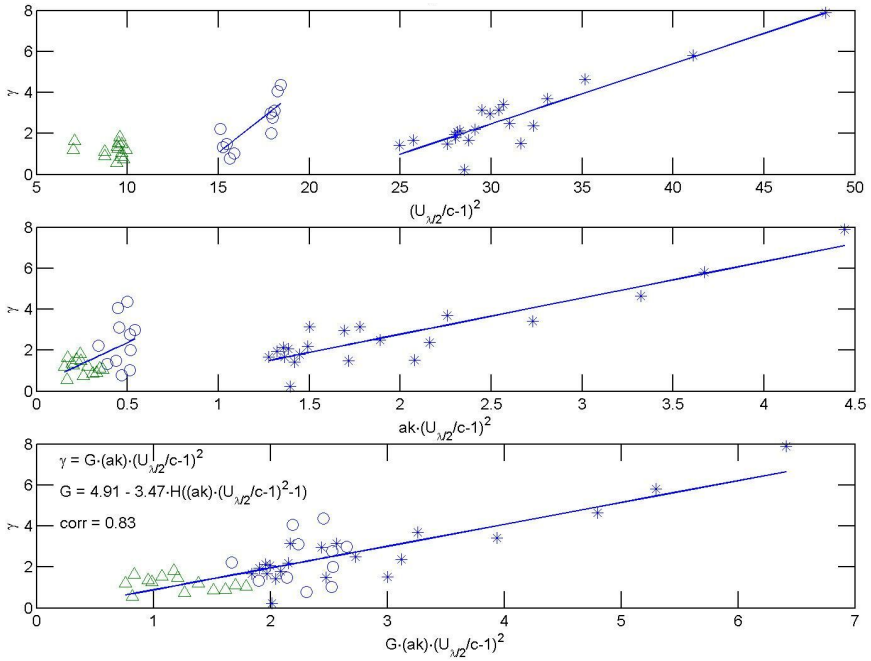

Figure 3. Dependence of the growth rate γ on the wind/steepness parameter. (top) Wind parameter is $(U_{\lambda/2} / c - 1)^2$. *The data cluster in three separate groups; (middle) Wind-steepness parameter is* $ak \cdot (U_{\lambda/2} / c - 1)^2$. *The data collapse into two groups; (bottom) Wind-steepness-separation parameter is* $G \cdot ak \cdot (U_{\lambda/2} / c - 1)^2$. *The data merge together. (Symbols denote the same data points in all three subplots).*

Clearly, the observed sheltering coefficients *s* depend on *ak* and this parameter was incorporated in the middle panel of Fig. 3 where dependence of γ on $ak(U_{\lambda/2} / c - 1)^2$ is shown. The data designated by triangles and circles in the top panel now collapse into a common group. The two remaining clusters correspond to moderate winds (triangles and circles, $U_{10} < 10.8 m/s$) and high winds (asterisks, $U_{10} > 11.7 m/s$), and dependences drawn within each of the group intersect zero when either wind forcing of wave steepness become zero which again make them physically feasible.

Therefore, the fractional growth γ depends on steepness at each frequency, and thus on the wave spectrum. As a result, the wind input function (3) becomes a nonlinear function of spectrum *F(ω)*. This feature has not been present in the existing input spectral terms. Since typically the variation of

wave steepness in the ocean is small, such dependence for γ may not play an essential role in most of the circumstances, but obviously its absence limits the performance of the standard input terms in conditions when the change of the steepness is significant.

2.1.2. Relative reduction of the wind input at conditions of strong wind/ steep waves

In Fig. 3, it remained to understand why the steepness-dependent sheltering coefficient is different for the moderate and strong winds. Analysis conducted in Donelan et al. (2006) allowed to attribute this difference to the full air-flow separation at steep-wave/strong-wind conditions. For fast flows over steep wave crests, the vertical gradient of wave-induced pressure at the crest provides the centripetal acceleration to bend the streamlines over the crest and keep them in contact with the surface. Estimations of the balance of the centrifugal and centripetal forces revealed that if, for an individual wave, $ak(U_{\lambda/2}/c-1)^2>1$, flow separation occurs. For a particular wind speed, significance of the separation-effect contribution into the air-sea interaction will depend on a number of steep enough waves in the wave field.

The full separation of the flow over a steep wave crest means that the streamlines detach from the flow at the steep crest and do not reattach until well up the windward face of the preceding wave towards its crest. The consequence of this is that the shear layer, which is normally attached to the surface, moves upwards leaving a "dead zone" in the trough between crests. Thus the external flow skips over the wave troughs and the imposed pressure pattern is weaker than in the case with non-separated flow. However, the phase shift of the pressure maximum towards the re-attachment point on the windward face of the wave becomes bigger and it is not immediately obvious whether the combined effect will cause enhancement or reduction of the dimensionless wave growth.

Fig. 3 (middle) clearly exhibits drop of the sheltering coefficient once the onset of separation is reached. This separation effect was parameterised by means of a smoothed Heaviside function which provides a step-like transition between the two sheltering coefficients and brings all the data onto a single line in the bottom panel of Fig. 3. If translated into a form suitable for applications in spectral wave forecast models where information about steepness of individual waves is not available, the growth rate parameterisation is

$$\begin{aligned}\gamma &= G\sqrt{B_n}\left(\frac{U_{10}}{c}-1\right)^2,\\ G &= 2.80-1.00\cdot\tanh\left(10\sqrt{B_n}\left(\frac{U_{10}}{c}-1\right)^2-11\right).\end{aligned} \tag{6}$$

Here,

$$B_n(\omega)=\frac{\omega^5 F(\omega)}{2g^2} \tag{7}$$

is the dimensionless spectral saturation function introduced by Phillips (1985).

Thus, the flow separation results in a reduction of the wind input, but this reduction is relative. Overall, the wind input will keep growing as the wind speeds increase, but the rate of this growth, beyond the full separation onset, will be slower compared to straight extrapolations of the wind input functions obtained in the moderate-wind conditions.

At extreme wind conditions, i.e. U_{10} in excess of 30 m/s, sea drag C_d in (4) has been observed to saturate and even reduce (e.g. Powel et al., 2003, Powel, 2007, Holthuijsen et al., 2012). This signifies a relative reduction of the total stress (4), which is the integral of momentum flux from the wind to the waves across the spectrum. Such important element of the wind-input behaviour has attracted attention of the wave-modelling community and once again highlighted the necessity to validate and update the models' parameterisations against experimental knowledge and observations.

The drag-saturation effect at extreme winds resulted in a number of tuning modifications to the existing input terms in the wave models over the last decade, and a great number of theories appeared which offer possible explanations of the phenomenon. We refer the reader to a review of these theories in Babanin (2011b) who broadly subdivided them in four different classes according to the physics which they appeal to. Most often used physical mechanisms are the influences of spray on the wave boundary layer and the hydrodynamics effects at extreme winds. In this regard, the relative reduction of the wind input measured in Lake George and parameterised in (6) is purely due to hydrodynamics, as the measurements did not involve winds stronger than 12 m/s and the spray is not produced at such wind speeds. This parameterisation, however, if extrapolated to the hurricane wind speeds produces saturation of C_d at the level estimated by Powel et al. (2003), Powel (2007).

2.1.3. Role of the wave breaking in enhancing the wind input

Wave breaking is also known to instigate air-flow separation. Since the breaking becomes particularly frequent at extreme air-sea situations, it has a potential to significantly alter the wind-wave energy exchange in such circumstances. Based on Lake George data, this effect was investigated in detail first time in field conditions (Young and Babanin, 2001, Babanin et al., 2007b).

It was found that the flow separation induced by wave breaking has a different effect on wind input if compared to the 'full' separation. It does somewhat increase the phase shift of the induced-pressure maximum with respect to the wave trough, but the flow does not pass over the wave troughs altogether as in the case of the full separation, and the relative induced pressure does not drop but increases. This causes enhancement rather than reduction of the wave-induced pressure magnitude, plus the increased phase shift. Overall, the flow separation due to breaking always results in enhancement of the wind input.

The Lake George measurements allowed an assessment of the magnitude of the breaking-induced separation enhancement and provided a basis for parameterising the effect. Overall, this produced an enhanced wave-coherent energy flux from the wind to the waves with a mean value of 1.9 times the corresponding energy flux to the non-breaking waves. It was proposed that the breaking-induced enhancement of the wind input to the waves can be parameterised by the product of the non-breaking input and a function of breaking probability:

$$\gamma(\omega) = \gamma_0(\omega)\left(1 + b_T(\omega)\right) \tag{8}$$

Where γ_0 is the spectral wave growth rate increment in absence of wave breaking and b_T is the associated breaking probability per wave period. Here, γ, γ_0 and b_T are all spectral functions. Ultimately, if 100% of waves are breaking the effect can lead the wind input to double. In such extreme circumstances, however, physics of the air-sea interactions in general and of wave breaking in particular is expected to change (Babanin, 2011a,b, Holthuijsen et al., 2012).

b_T is essentially a crest count for breaking waves with respect to non-breaking waves, and respective pramteric dependences are available, for deep and finite-depth water, across a very wide range of conditions and spectral scales (Babanin et al., 2001, 2007c, Manasseh et al., 2006, Filipot et al., 2010, Babanin, 2011b). Such dependences allow both to estimate the contribution of breaking events to the wind input in (8) and to output the breaking rates based on forecast/hindcast of waves by spectral models.

2.2. Dissipation due to wave breaking

Spectral wave energy dissipation represents the least understood part of the physics relevant to wave modelling (e.g. Babanin, 2011b). There is a general consensus that the major part of this dissipation is supported by wave breaking. Understanding of physics of this breaking process has advanced significantly over the last decade, but measurements, modelling and theoretical description of the process, particularly for the spectral waves, is still in urgent need of attention.

Theoretical and experimental knowledge of the spectral wave dissipation is so insufficient that, to fill the gap, spectral models have been used to guess the spectral dissipation function D in (1) as a residual term of tuning the balance of better known source functions to fit known wave-spectrum features. This is the only source function in (1) which has until recently been inferred indirectly by modelling the evolution of the wave spectrum rather than by parameterising measured physical features.

As a result of Lake George experiment, spectral distribution of the wave-energy dissipation was directly measured. Two different methodologies were used to investigate the dissipation function. The first employed the acoustic noise spectrograms in order to identify segments of breaking and non-breaking dominant wave trains (Babanin et al., 2001). As a result, threshold-like behaviour of the breaking probability was revealed. If some characteristic wave steepness is below the threshold, the waves will not break (and whitecapping dissipation will be zero). If the steepness threshold is overcome, the breaking rates b_T are proportional to the steepness excess over this threshold, all squared.

The average power and directional spectra for breaking and non-breaking waves were obtained by the segmenting method, and the difference was attributed to the dissipation due to wave breaking (Babanin and Young, 2005, Young and Babanin, 2006). This method provides an estimate of the spectral effects, both in frequency and directional domains, of the dominant wave breaking.

As an independent second approach, a passive acoustic method of detecting individual bubble-formation events was developed. This method was found promising for obtaining both the rate of occurrence of breaking events at different wave scales and the severity of wave breaking (Manasseh et al., 2006). A combination of the two estimates should lead to direct estimates of the spectral distribution of wave dissipation.

If the wave energy dissipation at each frequency were due to whitecapping only, it should be a function of the excess of the spectral density above a dimensionless threshold spectral level, below which no breaking occurs at this frequency, as mentioned above. This was found to be the case around the wave spectral peak. A more complex mechanism appears to be driving the dissipation at scales different to those of the dominant waves. Dissipation at a particular frequency above the peak demonstrates a cumulative effect, depending on the integral over the spectrum at lower frequencies.

The nature of the induced dissipation above the peak can be due to either enhanced induced wave breaking (Manasseh et al., 2006, Young and Babanin, 2006), or modulation of short waves by longer waves (e.g. Longuet-Higgins and Stewart, 1960, Phillips, 1963, Donelan, 2001), or turbulent dissipation of short waves in the wake of a larger breaker (Banner et al., 1989). In terms of the dissipation function *D* such an effect will mean a two-phase behaviour: *D* being a simple function of the wave spectrum at the spectral peak and having an additional cumulative term at all frequencies above the peak.

The following parameterisation of the dissipation term was suggested:

$$D(\omega) = -a_1(\omega)\rho_w g\omega(F(\omega) - F_{thr}(\omega)) - a_2(\omega)\rho_w g\int_{\omega_p}^{\omega}(F(q) - F_{thr}(q))dq \qquad (9)$$

where ω_p is the spectral peak frequency, a_i are experimental constants, $F_{thr}(\omega)$ is the dimensional threshold. Initially, this formulation included normalisation by the value of directional spreading at each frequency, but later it was argued unnecessary (Babanin et al., 2007a, Babanin, 2011b). Coefficients a_1 and a_2 are not tuning parameters, but define/depend on relative importance of the inherent breaking and induced breaking/dissipation at a particular spectral scale. These relationships have been studied extensively and parameterised by Tsagareli (2009), Babanin et al. (2010), Rogers et al. (2012). Rogers et al. (2012) also suggested a dimensionless and nonlinear version of (8). The dimensional threshold $F_{thr}(\omega)$ at each frequency is obtained from the universal dimensionless value for the saturation spectrum (7) which is

$$\sqrt{2\pi B_n(\omega)} = const = 0.035 \qquad (10)$$

based on Lake George measurements (Babanin et al., 2010, Babanin, 2011b).

Young and Babanin (2006) also compared directional spectra of the breaking and post-breaking waves whose difference should be indicative of the directional distribution of the dissipation. They showed that directional dissipation rates at oblique angles are higher than the dissipation in the main wave-propagation direction and therefore the breaking tends to make the wave directional spectra narrower. This conclusion may have very significant implications for the directional shape of *D*: unlike *I*, it would be bimodal with respect to the wind direction, and the main wave direction would be characterised by a local minimum of the directional spectrum of dissipation.

Another feature of the spectral dissipation function, revealed by the Lake George studies, shows distinctiveness of the dissipation behaviour at strong winds. For the moderate wind, according to (9), the dissipation function is mainly determined by the wave spectrum. In these circumstances, the wind influence on wave breaking and energy attenuation is indirect: the wind changes the wave spectrum first, and this change brings about alterations of the breaking as a consequence. At strong winds of $U_{10} > 14m/s$, however, further increase of the wind speed and the wind input does not cause noticeable changes of the wave spectrum (2007a). The excessive wind input, or at least a significant part of that, appears to be dissipated locally through an enhanced breaking (see also discussions in Babanin (2011b)).

2.3. Interaction of waves with adverse wind

Negative wind input or, rather, wave energy dissipation due to interaction with the adverse winds is a phenomenon confirmed experimentally. If the observation-based functions described above are adopted, an additional energy sink has to be employed as this extra dissipation is not accommodated by either of them, and it is not small. Such dissipation does not necessarily require the wind at 180 degrees to the propagation direction of the dominant waves, but can occur elsewhere in the directional spectrum if any of such directional components has a wavenumber component negative with respect to an oblique wind speed vector.

Donelan (1999) explicitly and thoroughly measured this effect in a laboratory with wave-following facility:

$$\gamma = \begin{cases} 0.28(U_{\lambda/2}/c-1)\,|U_{\lambda/2}/c-1| & for \quad U_{\lambda/2}/c \geq 1, \\ 0.11(U_{\lambda/2}/c-1)\,|U_{\lambda/2}/c-1| & for \quad U_{\lambda/2}/c < 1. \end{cases} \tag{11}$$

Here, the wind input is described in terms of (5), with sheltering coefficient s=0.28 for the following wind and s=0.11 for the adverse wind. Thus, interaction with the adverse wind is 2.5 times weaker, for the same wind speed, but it is still very significant.

The issue of applying results of laboratory measurements to the field conditions has been a subject of considerable debate for a long time. In particular, the s=0.28 coefficient for the laboratory waves has been pointed out as a much stronger interaction property by comparison with field measurement of Hsio and Shemdin (1982) who obtained s=0.12 for the following winds. This seemed as an illustration of the fact that the laboratory measurements of wind-wave exchanges are not directly applicable to the ocean waves.

Donelan et al. (2006), however, reconciled this controversy. Sheltering coefficient in (6) depends on wave steepness and the flow-separation feature, in addition to the wind speed magnitude. Since the steepness of laboratory waves of Donelan (1999) is much larger than steepness of fully developed waves of Hsiao and Shemdin (1982), the general parameterisation (6) is able to accommodate both particular results.

Therefore, until comprehensive measurements of the negative wind input in field conditions are obtained, using parameterisation (6) with magnitude reduced according to (11) is a feasible option to describe interactions of the waves and opposing winds. Such conditions are difficult to capture and measure in the field, but observational guidance in this regard is available. Fig. 4 shows an almost 180-degree wind turn recorded at Lake George (left) and a respective drop of the significant wave height (right). In Fig. 5, wave spectra before (left) and after the turn (right) are plotted. The drop of the initial wave energy and growth of waves in the new direction is apparent. When employed in WAVEWATCH-III, the combined (6) and (11) positive and negative wind inputs are able to reproduce this situation (Zieger, private communication).

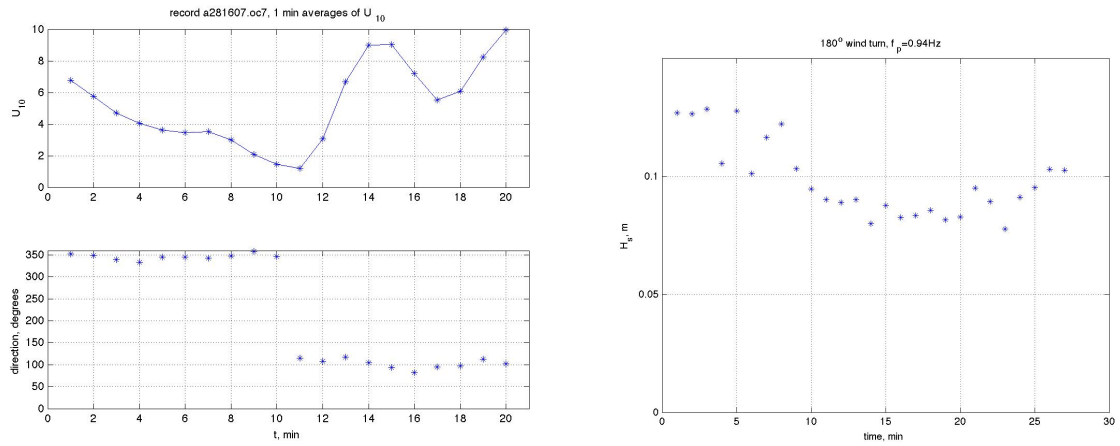

Figure 4. 180-degree wind turn recorded at Lake George. Bottom scale is time in minutes. (left) Wind speed (top) and wind direction (bottom). (right) Significant wave height H_s.

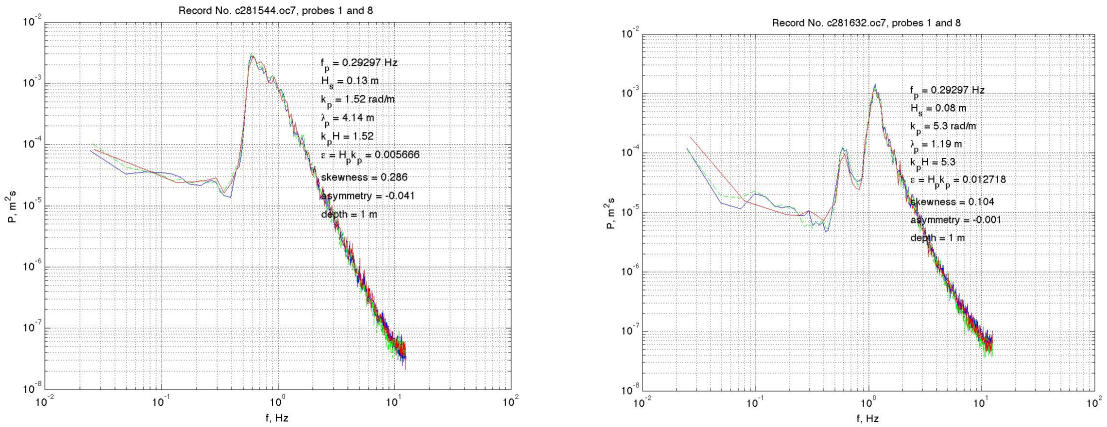

Figure 5. 180-degree wind turn recorded at Lake George. Bottom scale is frequency in Hz, vertical scale is spectral density in $m^2 s$ *. Wave spectra before (left) and after (right) the turn.*

3. Discussion and conclusions

In the paper, a suit of observation-based source functions for spectral models is reviewed, following existing publications. These are wind input, whitecapping dissipation and negative input (interaction of waves with adverse wind). New parameterisations are based on measurements and observations, which revealed new physics previously unaccounted for. For extreme conditions, physics of the wind input and whitecapping dissipation terms exhibit additional features irrelevant or inactive at moderate weather.

It is argued that experimental knowledge of the source terms is no longer fragmentary. The newly observed features for the wind input and wave-breaking dissipation are a certain observation-based knowledge. They may lead to different formulations and parameterisations of the source terms, but are necessary to be accommodated in the models for them to conform with the physical reality. Tuned models may perform very well, but are bound to biases and even possible failures beyond the range of their initial applicability. Besides, physics-based models allow for incremental, gradual and continuing improvements and updating, as opposed to re-tuning the entire set of terms should the new circumstances are to be accommodated.

Some other issues related to the physics of the modelling have been just briefly mentioned or left behind. Such is the problem of validating the source functions separately, rather than by means of verifications of their combined performance in a complex model. Experimental and theoretical knowledge and understanding of physical constraints in the wave system is available for such independent validations. For example, the integrated momentum input to the wave spectrum has to equal the wind stress known independently, and the integral of the dissipation terms is an experimentally known fraction of the input. The source terms calibrated before implementing in the model, ideally, should not require further tuning and instead should expose situations where the models' physics is inaccurate or inadequate.

Here, we concentrated on the wind-wave exchanges and wave-breaking dissipation. Not everything is known or even clear for these source terms. For example, the their directional distributions are included in every model, but for the wind input were never measured and for the dissipation have still not been documented in detail.

In the general circumstances, other terms are also of great significance. One of them is the dissipation of swell. Swells are ever present in the ocean spectra, and in some regions of the ocean they dominate the wave climate. Since dissipation rates for swell are small and therefore their decay spans tens of thousands of wave periods, it is very difficult to measure. Observations guidance here, however, also became available following satellite observations of Ardhuin et al. (2009) and new dissipation terms have been proposed. Ardhuin et al. (2009) describe the observed attenuation of swell in terms of inferred mechanism of wave interactions with the turbulent atmospheric boundary layer, and Babanin (2011b, 2012) by means of wave-turbulence interaction in the upper ocean. While important for the wave modelling, this kind of energy-exchange term extends the modelling topic much further, to the wave influences in the context of large-scale processes in the atmospheric boundary layer, in the upper ocean, and in the air-sea interaction.

Finally, we will summarise the new features of the spectral energy source/sink terms outlined in the paper. For the wind input, the wave growth term was shown to be a nonlinear function of wave steepness. Additionally, the wave breaking was found to enhance the wind input. Relative reduction of the wind input at strong-wind/steep-wave conditions was observed, due to full flow separation found at such circumstances. At strong wind forcing, this causes saturation of the sea drag. For a given wind speed, magnitude of the negative input is 2.5 times smaller than the respective magnitude of positive wind input.

The spectral distribution of whitecapping dissipation exhibits a threshold behaviour in terms of wave steepness. At a particular frequency, the breaking was demonstrated to cause energy damping in a broad spectral band above that frequency, and thus bring about cumulative dissipative effect towards waves of smaller scales. It was found that at moderate winds the dissipation is fully determined by the wave spectrum whereas at strong winds it is a function of the wind speed. Parameterisations of the observed effects in the form suitable for spectral wave models are available.

References

Ardhuin, F., Chapron, B., and Collard, F. 2009: Observation of swell dissipation across oceans. *Geophys. Res. Lett*., 36, doi:10.1029/2008GL037030, 4p

Ardhuin, F., Rogers, E., Babanin, A., Filipot, J.-F., Magne, R., Roland, A., van der Westhuysen, A., Queffeulou, P., Lefevre, J.-M., Aouf, L., and Collard, F., 2010: Semi-empirical dissipation source functions for ocean waves. Part I: definitions, calibration and validations. *J. Phys. Oceanogr.,* 40, 1917-1941

Babanin, A.V., Young, I.R., and Banner, M.L., 2001: Breaking probabilities for dominant surface waves on water of finite constant depth. *J. Geophys. Res.,* C106, 11659-11676

Babanin, A.V., and I.R. Young, 2005: Two-phase behaviour of the spectral dissipation of wind waves. *Proc. Ocean Waves Measurement and Analysis, Fifth Int. Symp. WAVES2005, 3-7 July, 2005, Madrid, Spain*, Eds. B. Edge and J.C. Santas, paper no.51, 11p

Babanin, A.V., Young, I.R., and Mirfenderesk, H., 2005: Field and laboratory measurements of wave-bottom interaction. *Proc. 17th Australasian Coastal and Ocean Eng. Conf. and 10th Australasian Port and Harbour Eng. Conf., 20-23 September 2005, Adelaide, South Australia*, Eds. M.Townsend and D.Walker, The Institution of Engineers, Canberra, Australia, 293-298

Babanin, A.V., Tsagareli, K.N., Young, I.R., and Walker, D. 2007a: Implementation of new experimental input/dissipation terms for modeling spectral evolution of wind waves. *Proc.* 10th *Int. Workshop on Wave Hindcasting and Forecasting and Coastal Hazards, Oahu, Hawaii, November*, *11-16, 2007*, 12p

Babanin, A.V., Banner, M.L., Young, I.R., and Donelan, M.A., 2007b: Wave follower measurements of the wind input spectral function. Part 3. Parameterization of the wind input enhancement due to wave breaking. *J. Phys. Oceanogr.*, 37, 2764–2775

Babanin, A.V., Young, I.R., Manasseh, R., and Schultz, E., 2007c: Spectral dissipation term for wave forecast models, experimental study. *Proc.* 10th *Int. Workshop on Wave Hindcasting and Forecasting and Coastal Hazards, Oahu, Hawaii, November*, *11-16, 2007*, 19p

Babanin, A.V., and Makin, V.K., 2008: Effects of wind trend and gustiness on the sea drag: Lake George study. *J. Geophys. Res., C*113, doi:10.1029/2007JC004233, 18p

Babanin, A.V., Tsagareli, K.N., Young, I.R., and Walker, D.J., 2010: Numerical investigation of spectral evolution of wind waves. Part 2. Dissipation function and evolution tests. *J. Phys. Oceanogr.,* 40, 667-683

Babanin, A.V., 2011a: Change of regime of air-sea interactions in extreme weather conditions. *Proc. 20th Australasian Coastal and Ocean Eng. Conf. and 13th Australasian Port and Harbour Eng. Conf., 28-30 September 2011, Perth, Western Australia,* 5p

Babanin, A.V., 2011b: *Breaking and Dissipation of Ocean Surface Waves*. Cambridge University Press, 480p

Babanin, A.V., 2012: Swell attenuation due to wave-induced turbulence. *Proc. ASME 2012 31st Int. Conf. on Ocean, Offshore and Arctic Eng. OMAE2012, July 1-6, 2012, Rio de Janeiro, Brasil*, 5p

Banner, M.L., Jones, I.S.F., and Trinder, J.C., 1989: Wavenumber spectra of short gravity waves. *J. Fluid Mech*., 198, 321–344

Donelan, M.A., 1999: Wind-induced growth and attenuation of laboratory waves. In *Wind-over-Wave Couplings. Perspective and Prospects*, Eds. S.G.Sajadi, N.H.Thomas, J.C.R.Hunt, Clarendon Press, Oxford, 183-194

Donelan, M.A., 2001: A nonlinear dissipation function due to wave breaking. In *ECMWF Workshop on Ocean Wave Forecasting, 2-4 July, 2001*, Series ECMWF Proceedings, 87-94

Donelan, M.A., Babanin, A.V., Young, I.R., Banner, M.L., and McCormick, C., 2005: Wave follower field measurements of the wind input spectral function. Part I. Measurements and calibrations. *J. Atmos. Oceanic Tech.,* 22, 799–813

Donelan, M.A., Babanin, A.V., Young, I.R., and Banner, M.L., 2006: Wave follower measurements of the wind input spectral function. Part 2. Parameterization of the wind input. *J. Phys. Oceanogr.*, 36, 1672-1688

Donelan, M.A., Curcic, M., Chen, S.S., and Magnusson, A.K., 2012: Modeling waves and wind stress. *J. Geophys. Res.*, in press

Filipot, J.-F., Ardhuin, F., and Babanin, A.V., 2010: A unified deep-to-shallow-water spectral wave-breaking dissipation formulation. *J. Geophys. Res.,* C115, doi:10.1029/2009JC005448, 15p

Hasselmann, K., 1960: Grundleiehungen der Seegangsvoraussage. *Schiffstechnik*, v.7, 191-195

Hasselmann, K., Barnett, T.P., Bouws, E., Carlson, H., Cartwright, D.E., Enke, K., Ewing, J.A., Gienapp, H., Hasselmann, D.E., Kruseman, P., Meerburg, A., Muller, P., Olbers, D.J., Richter, K., Sell, W., and Walden, H., 1973: Measurements of wind-wave growth and swell decay during the Joint North Sea Wave Project (JONSWAP). *Dtsch. Hydrogh. Z. Suppl*., A8(12), 1-95

Holhuijsen, L.H., Powel, M.D., and Pietrzak, J.D., 2012: Wind and waves in extreme hurricanes. *J. Geophys. Res.*, in press

Hsiao, S.V., and Shemdin, O.H., 1983: Measurements of wind velocity and pressure with wave follower during MARSEN. *J. Geophys. Res*., 88, 9841-9849

Komen, G.I., Cavaleri, L., Donelan, M., Hasselmann, K., Hasselmann, S., and Janssen, P.A.E.M., 1994: *Dynamics and Modelling of Ocean Waves*. Cambridge University Press, UK, 554p

Longuet-Higgins, M.S., and Stewart, R.W., 1960: Changes in the form of short gravity waves on long waves and tidal currents. *J. Fluid Mech*., 8, 564-585

Manasseh, R., Babanin, A.V., Forbes, C., Rickards, K., Bobevski, I., and Ooi, A., 2006: Passive acoustic determination of wave-breaking events and their severity across the spectrum. *J. Atmos. Oceanic Tech.,* 23, 599–618

Mitsuyasu, H., 1971: On the form of fetch-limited wave spectrum. *Coastal Eng. Japan*, v.14, 7-14

Phillips, O.M., 1963: On the attenuation of long gravity waves by short breaking waves. *J. Fluid Mech.*, 16, 321-332

Phillips, O.M., 1985: Spectral and statistical properties of the equilibrium range of wind-generated gravity waves. *J. Fluid Mech*., 156, 505-531

Powel, M.D., Vickery, P.J., and Reinhold, T.A., 2003: Reduced drag coefficient for high wind speeds in tropical cyclones. *Nature*, 422, 279-283

Powell, M.D., 2007: Drag coefficient distribution and wind speed dependence in tropical cyclone. *Final Report to the National Oceanic \& Atmospheric Administration*, Joint Hurricane Testbed Program, 26p

Rogers, W.E., Babanin, A.V., and Wang, D.W., 2012: Observation-consistent input and whitecapping-dissipation in a model for wind-generated surface waves: Description and simple calculations. *J. Atmos. Oceanic Tech.*, in press

Tolman, H.L., Banner, M.L., and Kaihatu, J.M., 2011: The NOPP operational wave model improvement project. *Proc. 12th Int. Workshop on Wave Hindcasting and Forecasting and 3rd Coastal Hazards Symp., Big Island, Hawaii, October 30 –November 4*, 19p

Tsagareli, K.N., Babanin, A.V., Walker, D.J., and Young, I.R., 2010: Numerical investigation of spectral evolution of wind waves. Part 1. Wind input source function. *J. Phys. Oceanogr.,* 40, 656-666

WISE Group, The: Cavaleri, L., Alves, J.-H.G.M., Ardhuin, F., Babanin, A., Banner, M., Belibassakis, K., Benoit, M., Donelan, M., Groeneweg, J., Herbers, T.H.C, Hwang, P., Janssen, P.A.E.M., Janssen, T., Lavrenov, I.V., Magne, R., Monbaliu, J., Onorato, M., Polnikov, V., Resio, D., Rogers, W.E., Sheremet, A., McKee Smith, J., Tolman, H.L., van Vledder, G., Wolf, J., and Young, I., 2007: Wave modelling - The state of the art. *Progr. Oceanogr*., 75, 603-674

Young, I.R., and Babanin, A.V., 2001: Wind wave evolution in finite depth water. *Proc. 14th Australasian Fluid Mech. Conf.*, *2001, Adelaide, Australia,* 79-86

Young, I.R., Banner, M.L., Donelan, M.A., Babanin, A.V., Melville, W.K., Veron, F., and McCormick, C. 2005: An integrated system for the study of wind wave source terms in finite depth water. *J. Atmos. Oceanic Tech.,* 22, 814–828

Young, I.R., and Babanin, A.V., 2006: Spectral distribution of energy dissipation of wind-generated waves due to dominant wave breaking. *J. Phys. Oceanogr.*, 36, 376–394

Zieger, S., Babanin, A.V., Rogers, W.E., and Young, I.R., 2011: Observation-based dissipation and input terms for WAVEWATCH III™: implementation and simple simulations. *Proc. 12th Int. Workshop on Wave Hindcasting and Forecasting and 3rd Coastal Hazards Symp., Big Island, Hawaii, October 30 –November 4*, 12p